Methylenetetrahydrofolate Reductase from *Escherichia coli*: Elucidation of the Kinetic Mechanism by Steady-State and Rapid-Reaction Studies†

Elizabeth E. Trimmer,‡ David P. Ballou, and Rowena G. Matthews*

Department of Biological Chemistry and Biophysics Research Division, The University of Michigan, Ann Arbor, Michigan 48109-1055

Received December 8, 2000; Revised Manuscript Received March 20, 2001

ABSTRACT: The flavoprotein methylenetetrahydrofolate reductase (MTHFR) from *Escherichia coli* catalyzes the reduction of 5,10-methylenetetrahydrofolate (CH_2-H_4folate) to 5-methyltetrahydrofolate (CH_3-H_4folate) using NADH as the source of reducing equivalents. The enzyme also catalyzes the transfer of reducing equivalents from NADH or CH_3-H_4folate to menadione, an artificial electron acceptor. Here, we have determined the midpoint potential of the enzyme-bound flavin to be −237 mV. We have examined the individual reductive and oxidative half-reactions constituting the enzyme's activities. In an anaerobic stopped-flow spectrophotometer, we have measured the rate constants of flavin reduction and oxidation occurring in each half-reaction and have compared these with the observed catalytic turnover numbers measured under steady-state conditions. We have shown that, in all cases, the half-reactions proceed at rates sufficiently fast to account for overall turnover, establishing that the enzyme is kinetically competent to catalyze these oxidoreductions by a ping-pong Bi−Bi mechanism. Reoxidation of the reduced flavin by CH_2-H_4folate is substantially rate limiting in the physiological NADH-CH_2-H_4folate oxidoreductase reaction. In the NADH-menadione oxidoreductase reaction, the reduction of the flavin by NADH is rate limiting as is the reduction of flavin by CH_3-H_4folate in the CH_3-H_4folate-menadione oxidoreductase reaction. We conclude that studies of individual half-reactions catalyzed by *E. coli* MTHFR may be used to probe mechanistic questions relevant to the overall oxidoreductase reactions.

Methylenetetrahydrofolate reductase (MTHFR)[1] is a flavoprotein that catalyzes the reduction of 5,10-methylenetetrahydrofolate (CH_2-H_4folate) to 5-methyltetrahydrofolate (CH_3-H_4folate), as shown in eq 1.

$$CH_2\text{-}H_4\text{folate} + NAD(P)H + H^+ \rightarrow CH_3\text{-}H_4\text{folate} + NAD(P)^+ \quad (1)$$

In the reaction, NAD(P)H transfers reducing equivalents to a noncovalently bound flavin adenine dinucleotide (FAD) cofactor, which in turn transfers them to CH_2-H_4folate. MTHFR provides CH_3-H_4folate for use in the methylation of homocysteine to form methionine. In humans, mutations in MTHFR have been correlated with elevated levels of homocysteine, a risk factor for cardiovascular disease (*1*, *2*) and with neural-tube defects in the fetus (*3*−*5*).

MTHFR from porcine liver has been purified and extensively characterized (reviewed in ref *6*). Using peptide sequences from the porcine enzyme, a cDNA for the human enzyme was identified and sequenced (*7*). Eukaryotic MTHFRs are homodimeric enzymes in which each subunit is composed of an N-terminal catalytic domain and a C-terminal regulatory domain. The subunits of MTHFRs from enteric bacteria contain only the catalytic domain and alignment of their sequences with the catalytic domains of the eukaryotic enzymes shows a ∼30% sequence identity. This level of sequence identity predicts that the enzymes will have both structural and mechanistic similarities.

Our studies have recently focused on *Escherichia coli* MTHFR as a model for the catalytic domain of the human enzyme. The X-ray structure of the *E. coli* enzyme has been determined (*8*). In contrast to the porcine and human enzymes, which are available only in limited quantities, *E. coli* MTHFR has been overexpressed and homogeneous protein can be obtained in high yields (*9*). The availability of this enzyme and the determination of its structure make it ideal for investigation of the chemical and kinetic mechanism as well as for examination of the catalytic roles of specific amino acid residues. In an earlier paper, we described the initial characterization of the *E. coli* enzyme (*9*). The properties of *E. coli* MTHFR are similar to those of the porcine enzyme. The *E. coli* enzyme, however, uses NADH in preference to NADPH, whereas the porcine enzyme uses NADPH preferentially. The kinetic analysis of porcine MTHFR is complicated because of the allosteric inhibition of enzyme activity by adenosylmethionine (AdoMet) (*10*, *11*). Even in the absence of AdoMet, approximately 25% of

† This work was supported in part by National Institutes of Health Research Grants GM24908 (R.G.M.) and GM20877 (D.P.B.). E.E.T. was supported in part by an NIH postdoctoral fellowship (GM19816).

* To whom correspondence should be addressed. E-mail: rmatthew@umich.edu. Phone: (734) 764-9459. Fax: (734) 764-3323.

‡ Present address: Department of Chemistry, Grinnell College, Grinnell, IA 50112.

[1] Abbreviations: AdoMet, adenosylmethionine; CH_2-H_4folate, 5,10-methylenetetrahydrofolate; CH_3-H_4folate, 5-methyltetrahydrofolate; *E. coli*, *Escherichia coli*; EDTA, ethylenediaminetetraacetic acid; E_m, midpoint potential; FAD, flavin adenine dinucleotide; MTHFR, methylenetetrahydrofolate reductase; PCA, protocatechuate; PCD, protocatechuate dioxygenase; H_4folate, tetrahydrofolate.

10.1021/bi002789w CCC: $20.00
Published on Web 05/01/2001

the enzyme is in the inactive T state, and slow interconversion of the inactive T state enzyme to the active R state occurs when NADPH is added (*11*). In contrast, there is no evidence that the *E. coli* enzyme is subject to allosteric regulation by AdoMet.

In addition to the physiological oxidoreductase reaction, MTHFR catalyzes the reactions shown in eqs 2 and 3, in which menadione is used as an artificial electron acceptor.

$$\text{NAD(P)H} + \text{menadione} \rightarrow \text{NAD(P)}^{+} + \text{menadiol} \quad (2)$$

$$\text{CH}_3\text{-H}_4\text{folate} + \text{menadione} \rightarrow \text{CH}_2\text{-H}_4\text{folate} + \text{menadiol} \quad (3)$$

These assays have the virtue of being conducted in air saturated buffers, because the reaction of reduced enzyme with oxygen is much slower than its reaction with menadione; in contrast, the physiological oxidoreductase assay (eq 1) can only be conducted under anaerobic conditions, due to the susceptibility of CH_2-H_4folate to oxidation. Porcine MTHFR has been shown to catalyze the reactions shown in eqs 1−3 by employing ping-pong Bi−Bi mechanisms (*12*, *13*), in which the enzyme-bound FAD is alternately reduced by one substrate and oxidized by the second substrate. Preliminary data suggest a similar mechanism for the *E. coli* enzyme. Each of the catalytic reactions shown in eqs 1−3 can be divided into two half-reactions that can be examined individually: a reductive half-reaction in which the enzyme-bound FAD is reduced and an oxidative half-reaction in which the reduced FAD is reoxidized. Before basing mechanistic conclusions about the overall catalytic reaction on observations derived from the study of individual half-reactions, however, it is important to demonstrate for the *E. coli* enzyme that the half-reactions are kinetically competent for normal catalysis, i.e., that they proceed at rates sufficiently fast to account for overall turnover.

In the present study, we have investigated the catalytic properties of *E. coli* MTHFR. We have measured the steady-state kinetic parameters for the reactions shown in eqs 1−3. We have also examined, under the same experimental conditions, the individual half-reactions associated with these activities, by measuring the rate constants of flavin reduction and oxidation under anaerobic conditions in a stopped-flow spectrophotometer. We have demonstrated the formation of pre-steady-state enzyme−substrate complexes for the first time. We have also shown that in all cases, the half-reactions occur at rates sufficiently rapid to account for overall catalytic turnover. We conclude that *E. coli* MTHFR is kinetically competent to catalyze these overall reactions by ping-pong Bi−Bi mechanisms. In the following paper in this issue, we apply these kinetic methods to the characterization of two mutant enzymes in order to probe the roles of specific residues in the chemical mechanism of this important enzyme.

EXPERIMENTAL PROCEDURES

Materials. NADH, menadione, FAD, dimedone, phenosafranine, benzyl viologen, xanthine, and protocatechuate (3,4-dihydroxybenzoate) were purchased from Sigma. Formaldehyde was obtained from Fisher. [5-^{14}C-*methyl*]-(6*R*,*S*)-CH_3-H_4folate (specific activity 54 mCi mmol^{-1}) was purchased from Amersham Pharmacia Biotech as the barium salt. Nonradioactive (6*R*,*S*)-CH_3-H_4folate (calcium salt) was purchased from Schircks Laboratories (Jona, Switzerland). (6*S*)-CH_3-H_4folate and (6*S*)-H_4folate (sodium salts) were gifts from Eprova (Schaffhausen, Switzerland). Xanthine oxidase and 3,10-dimethyl-5-deazaisoalloxazine were provided by V. Massey. Protocatechuate dioxygenase (PCD) was purified from *Pseudomonas cepacia* DB01 (*14*). The Econo-Pac DG-10 columns were purchased from Bio-Rad.

Concentrations of the following solutions were determined spectrophotometrically using published extinction coefficients: $\epsilon_{340} = 6230$ M^{-1} cm^{-1} for NADH (*15*), $\epsilon_{340} = 3100$ M^{-1} cm^{-1} for menadione in methanol (*13*, *16*), $\epsilon_{290} = 31\,700$ M^{-1} cm^{-1} (pH 7.2) for CH_3-H_4folate (*17*), $\epsilon_{297} = 32\,000$ M^{-1} cm^{-1} (pH 7.2) for CH_2-H_4folate (*17*), $\epsilon_{298} = 28\,400$ M^{-1} cm^{-1} (pH 7.2) for H_4folate (*17*).

E. coli MTHFR Purification. E. coli MTHFR modified with a six-histidine tag on the C-terminus was expressed and purified by a published procedure (*9*) or by a slightly modified version. In the modified method, the nickel affinity chromatography was carried out with buffer solutions containing 10% glycerol. The fractions containing pure enzyme, as assessed by polyacrylamide gel electrophoresis in the presence of sodium dodecyl sulfate, were pooled and concentrated with Centricon 100 microconcentrators (Millipore). The buffer was exchanged to 50 mM potassium phosphate (pH 7.2) containing 0.3 mM EDTA and 10% glycerol by gel filtration chromatography on a DG-10 column (Bio-Rad). The protein was stored at −80 °C at a concentration of greater than 300 μM. Using the above procedure for purification, a liter of cell culture yielded greater than 60 mg of purified MTHFR. Enzyme concentrations were determined from the visible absorbance at 447 nm due to bound FAD, using a molar absorbance coefficient of 14 300 M^{-1} cm^{-1} (*9*). Throughout this paper, the enzyme concentration has been expressed as the molarity of enzyme-bound FAD; the enzyme (a tetramer) contains one molecule of FAD per subunit of 34 062 Da (*9*).

Methods. All experiments were conducted at 25 °C in 50 mM potassium phosphate (pH 7.2) containing 0.3 mM EDTA and 10% glycerol (referred to as protein buffer), unless otherwise noted. UV−vis spectra were recorded with a Shimadzu UV2501PC double-beam spectrophotometer or a Hewlett-Packard 8453 diode array spectrophotometer.

Midpoint Potential Determination. The midpoint potential of the enzyme-bound FAD of *E. coli* MTHFR was determined spectrophotometrically by employing the xanthine/xanthine oxidase reducing system with benzyl viologen as mediator (*18*). Phenosafranine was used as the reference redox dye of known potential. The E_m for the phenosafranine redox couple is −252 mV at pH 7.0 (*15*), and at pH 7.2, E_m is calculated to be −258 mV (*19*). A 1.40 mL solution of 20 μM enzyme, 300 μM xanthine, 2 μM benzyl viologen, and 10 μM phenosafranine was placed in an anaerobic cuvette with two sidearms similar to that previously described (*20*). Xanthine oxidase (6 μL of a 25 μM solution, 100 nM final concentration) was put in a sidearm. The contents of the cuvette were made anaerobic by 10 cycles of alternate evacuation and equilibration with high-quality argon that had been further purified by passage over an oxygen-absorbing gas purifier (LabClear). After the solution was made anaerobic, xanthine oxidase was tipped in to start the reaction. The time-dependent reduction of the enzyme and dye was

followed by monitoring changes in the absorbance spectrum between 300 and 800 nm. Complete reduction of the system was achieved in 1 h; longer reduction times resulted in substantial turbidity due to precipitation of enzyme upon reduction. The reduction of the redox dye phenosafranine was monitored by the decrease in absorbance at 520 nm, where neither the oxidized nor reduced enzyme forms absorb, and the reduction of enzyme was monitored by the decrease in absorbance at 398 nm, which is isosbestic for the reduction of phenosafranine. The ratios of oxidized and reduced enzyme or dye were calculated from each spectrum, and the log(ox/red) of the dye was plotted versus the log(ox/red) of the enzyme-bound FAD, according to the method of Minnaert (*21*). The change in midpoint potential (ΔE_m) between the reference dye and the enzyme-bound FAD was determined from the value of log(ox/red) of the enzyme at the point where log(ox/red) of the dye was zero. Then, using a midpoint potential of −258 mV for the phenosafranine couple at pH 7.2 (*15*, *19*), the midpoint potential of the enzyme-bound FAD was calculated (*21*).

Stopped-Flow Measurements of Enzymatic Half-Reactions. Rapid-reaction measurements were performed in a Hi-Tech Scientific SF-61 stopped-flow spectrophotometer equipped with a tungsten light source for single wavelength detection. For anaerobic work, the instrument was flushed with an oxygen-scrubbing solution of 0.1 M potassium phosphate (pH 7) containing protocatechuate dioxygenase (PCD) (∼0.1 unit mL^{-1}) and its substrate, protocatechuate (PCA, 3,4-dihydroxybenzoate) (200 μM), and allowed to stand overnight (*22*). For each experiment, a solution of 20 μM enzyme and 200 μM PCA was placed in a glass tonometer, with PCD in a sidearm. The contents of the tonometer were made anaerobic by 10 cycles of evacuation followed by equilibration with oxygen-free argon. At completion of the gas exchanges, PCD (∼0.1 unit mL^{-1} final concentration) was introduced from the sidearm. When reduced enzyme was used for experiments, the enzyme solution also contained 10 mM EDTA and 2 μM 3,10-dimethyl-5-deazaisoalloxazine. Following the deoxygenation cycles, the enzyme, while immersed in an ice water bath, was photoreduced (*23*) by exposure to visible light from a Sun Gun (Smith Victor Corp., Griffith, IN) for 1−2 min. PCD (∼0.1 unit mL^{-1} final concentration) was then introduced from a sidearm, which had been shielded from light. Control experiments indicated that the PCD/PCA oxygen-scavenging system had no effect on the measured rate constants.

Substrate solutions containing various concentrations of NADH, (6*S*)-CH_3-H_4folate, or menadione were prepared in the protein buffer and bubbled with oxygen-free argon for 10 min. PCA and PCD were added as an oxygen-scavenging system just prior to use. A (6*R*)-CH_2-H_4folate stock solution was prepared anaerobically by adding 15 mg of (6*S*)-H_4folate to 5 mL of deaerated 50 mM potassium phosphate buffer (pH 8.6) containing 10% glycerol and 0.3 mM EDTA. Formaldehyde (50 μL of a 6.2 M stock, 10-fold molar excess) was added to generate 6 mM (6*R*)-CH_2-H_4folate, and the solution was kept on ice under positive pressure under argon. Substrate solutions containing (6*R*)-CH_2-H_4folate were made by adding various amounts of the (6*R*)-CH_2-H_4folate stock solution to deaerated protein buffer. All solutions were brought to a final concentration of 2 mM formaldehyde (after mixing), and then PCA and PCD were added. Control experiments performed without added formaldehyde yielded results similar to those obtained with solutions containing 2 mM formaldehyde.

Reduction of the enzyme-bound FAD or reoxidation of reduced enzyme was followed at 450 nm. Transient charge-transfer complexes between enzyme-bound FAD and pyridine nucleotide were monitored at 550 and 650 nm. Rate constants were calculated from exponential fits of single-wavelength absorbance traces using the program KISS (Kinetic Instruments, Inc.), which employs the Marquardt−Levenberg algorithm (*24*). In most cases, the values calculated for the observed rate constants demonstrated a hyperbolic dependence on the substrate concentration. Using a nonlinear least-squares fitting algorithm in the program Kaleidagraph (Synergy Software, Reading, PA), the data were fit to eq 4

$$k_{obs} = \frac{k_{max}[S]}{K_d + [S]} \quad (4)$$

where k_{obs} is the observed rate constant, k_{max} is the maximum rate constant at saturating substrate, [S] is the concentration of substrate, and K_d is the apparent dissociation constant for the enzyme−substrate complex. In these determinations, however, the true dissociation constant is likely less than the calculated apparent K_d value because at concentrations of substrate (10−25 μM) comparable to the 10 μM enzyme concentration, the concentration of free substrate is less than the concentration of total substrate. Furthermore, under these conditions, reactions are not truly first order.

Steady-State Kinetic Assays. (i). CH_3-H_4folate-Menadione Oxidoreductase Assay. Using menadione as an alternative electron acceptor, MTHFR oxidizes [5-^{14}C-*methyl*] CH_3-H_4folate to [5-^{14}C-*methylene*] CH_2-H_4folate, which breaks down in the presence of acid and heat to $^{14}CH_2O$ (formaldehyde) and H_4folate (*25*, *26*). For quantitation, the radiolabeled formaldehyde is complexed with dimedone, extracted into toluene, and measured by scintillation counting. The assay was performed as described previously (*9*), except with the following modifications. All reactions were carried out at 25 °C and pH 7.2. The reaction mixture (820 μL) contained 50 mM potassium phosphate (pH 7.2), 0.3 mM EDTA, 10% glycerol, 0.24% bovine serum albumin, 37 μM FAD, 140 μM menadione, and [5-^{14}C-*methyl*] (6*R*,*S*)-CH_3-H_4folate (specific activity 1200 dpm $nmol^{-1}$) at a range of concentrations from 17 to 507 μM (6*S*)-CH_3-H_4folate. The mixture was preincubated at 25 °C for 5 min, and the reaction was initiated by addition of 20 μL of enzyme (final concentration 0.72 μM). The enzyme was stored in stock solutions of 29 μM prior to dilution into the assay mixtures. After 30 s, the assay was terminated by the addition of 300 μL of 3 mg mL^{-1} dimedone in 1 M sodium acetate (pH 4.5) and incubated at 100 °C for 2 min. The reaction mixtures were cooled on ice for 2 min and 3 mL of toluene were added. The mixture was vortexed until well-mixed and then spun in a clinical centrifuge at 3700 rpm for 8 min. A 1 mL volume of the toluene phase was added to 10 mL of Ecolite scintillation cocktail (ICN Biomedicals Inc.) and counted. All assays were corrected for the cpm found in samples to which buffer was added in place of enzyme. Using the program Kaleidagraph, the v/E_T versus (6*S*)-CH_3-H_4folate data were fit to the Michaelis−Menten kinetic equation (eq

5) to obtain the steady-state kinetic parameters K_m and k_{cat}.

$$\frac{v}{E_T} = \frac{k_{cat}[S]}{K_m + [S]} \quad (5)$$

(ii) NADH-Menadione Oxidoreductase Assay. In the presence of menadione, MTHFR oxidizes NADH to NAD^+ and the reaction can be monitored by the decrease in the NADH absorbance at 343 nm (*25*, *26*). The assay was performed as described previously (*9*), except with the following modifications. To determine the K_m for NADH, a 3 mL reaction mixture containing 50 mM potassium phosphate (pH 7.2), 0.3 mM EDTA, 10% glycerol, 140 μM menadione, and 5−300 μM NADH was preincubated at 25 °C for 5 min, and the reaction was initiated by addition of 5 μL of enzyme (final concentration 0.0167 μM). The enzyme was stored in stock solutions of 10 μM prior to dilution into the assay mixtures. Similarly, at an NADH concentration of 125 μM, menadione was varied from 5 to 140 μM to determine its K_m. As described by Daubner and Matthews (*12*), initial rates were calculated from the decrease in NADH absorbance at 343 nm over time, using an extinction coefficient of 6220 M^{-1} cm^{-1} for NADH. The 343 nm wavelength was chosen because oxidized menadione and its reduced form, menadiol, are isosbestic here and thus do not contribute to the observed absorbance changes. All assays were corrected for the initial rate observed in reaction mixtures to which buffer was added in place of enzyme. To correct the steady-state kinetic constants for inhibition due to excess NADH substrate, the data were fitted to eq 6 for single substrate inhibition in a ping-pong Bi−Bi system (*27*) using the program Kaleidagraph.

$$\frac{v}{E_T} = \frac{[A][B]k_{cat}}{K_{mB}[A](1 + [A]/K_{iA}) + K_{mA}[B] + [A][B]} \quad (6)$$

(iii) NADH-CH_2-H_4folate Oxidoreductase Assay. In the physiological NADH-CH_2-H_4folate oxidoreductase assay, MTHFR oxidizes NADH and reduces CH_2-H_4folate to CH_3-H_4folate. The oxidation of NADH can be observed as a decrease in the absorbance at 340 nm (*10*, *26*). The assay was performed as described previously (*9*), with modifications. All reactions were carried out at 25 °C and pH 7.2. Because of the susceptibility of CH_2-H_4folate to oxidation and to permit use of a higher concentration of enzyme, the assay was performed under anaerobic conditions in a stopped-flow instrument. We used a Hi-Tech Scientific SF-61 spectrophotometer equipped with a deuterium light source. Because of issues of enzyme stability upon dilution (*8*, *9*), a MTHFR concentration of 2.5 μM, prior to mixing, was employed in the experiments. Using the NADH-menadione and CH_2-H_4folate-menadione oxidoreductase assays, we determined that a 2.5 μM enzyme solution was stable over a time period of at least 6 h, sufficient time to perform the stopped-flow experiments (data not shown). MTHFR (2.5 μM) was mixed with an equal volume of buffer containing NADH and (6*R*)-CH_2-H_4folate. Prior to mixing, both solutions were deaerated, and PCA and PCD were added to scavenge any remaining oxygen. For use in these experiments, a (6*R*)-CH_2-H_4folate stock solution was prepared anaerobically from reaction of (6S)-H_4folate with formaldehyde as described above.

To determine the K_{mA} and K_{iA} for NADH, enzyme (1.25 μM after mixing) was mixed with an equal volume of solution containing 200 μM (6*R*)-CH_2-H_4folate and concentrations of NADH varying from 2.5 to 300 μM (concentrations after mixing). The K_{mB} and K_{iB} for CH_2-H_4folate were also determined using the NADH-CH_2-H_4folate oxidoreductase assay. Enzyme (1.25 μM after mixing) was mixed with an equal volume of solution containing 100 μM NADH and concentrations of (6*R*)-CH_2-H_4folate varying from 2 to 1000 μM (concentrations after mixing). Initial rates were calculated from the decrease in NADH absorbance over time, using an extinction coefficient of 6230 M^{-1} cm^{-1} for NADH at 340 nm (*15*). The steady-state kinetic parameters were determined by fitting the data to eq 7 for double substrate inhibition in a ping-pong Bi−Bi system (*27*) using the program Kaleidagraph. Because of the relatively high concentration of enzyme necessary for these experiments, the two lowest concentrations of substrate employed were only 2−5-fold higher than that of the enzyme, conditions out of the range of typical steady-state kinetics. Fits of the data with and without these lowest data points yielded similar kinetic parameters, within the allowed error of the experiment.

$$\frac{v}{E_T} = \frac{[A][B]k_{cat}}{K_{mA}[B](1 + [B]/K_{iB}) + K_{mB}[A](1 + [A]/K_{iA}) + [A][B]} \quad (7)$$

RESULTS

Midpoint Potential. The midpoint potential (E_m) of an enzyme is a measure of the potential required to form equal concentrations of oxidized and reduced enzyme forms. Typically, a bound flavin has a midpoint potential associated with one-electron reduction to the semiquinone and another midpoint potential associated with conversion of the semiquinone to the two-electron reduced hydroquinone. A semiquinone species of the flavin is not observed by either substrate- or photoreduction of *E. coli* MTHFR (data not shown), and therefore, a single midpoint potential for two-electron flavin reduction is determined. A method developed by Massey (*18*) was employed for measurement of the *E. coli* MTHFR midpoint potential. A representative experiment is shown in Figure 1A. Enzyme in equilibrium with phenosafranine, a redox dye with a midpoint potential of −258 mV at pH 7.2 (*15*, *19*), was reduced slowly by xanthine oxidase and its substrate xanthine. Benzyl viologen at a low concentration was included in the mixture to mediate electron transfer between xanthine oxidase, MTHFR, and phenosafranine. The reduction was monitored spectrally, and the spectra were analyzed for the concentrations of oxidized and reduced dye and the concentrations of oxidized and reduced MTHFR. A plot of the data according to the method of Minnaert (*21*) (Figure 1B) yielded a potential of −237 ± 4 mV for the enzyme redox couple. Similar results were obtained from two other experiments.

MTHFR Steady-State Assays and Half-Reactions. The catalytic properties of *E. coli* MTHFR have been defined by studying the three oxidoreductions catalyzed by the enzyme and the half-reactions constituting these oxidoreduc-

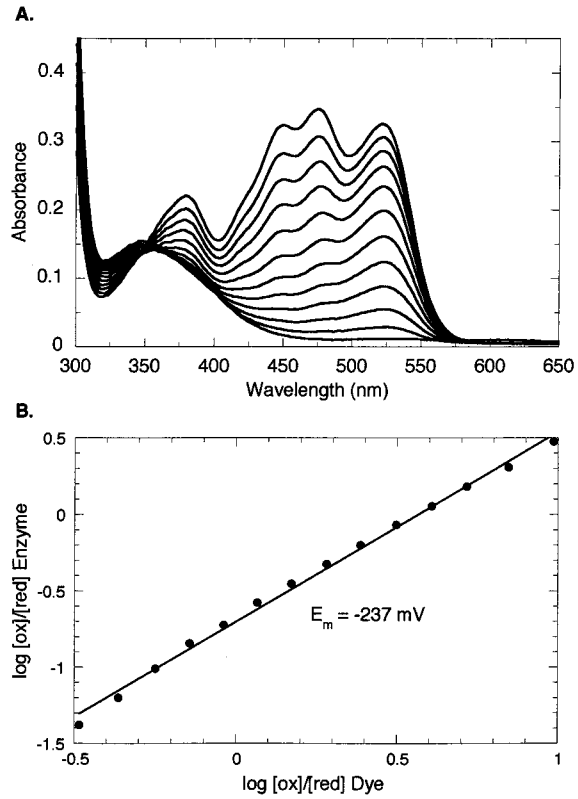

FIGURE 1: Determination of the midpoint potential of *E. coli* MTHFR. Anaerobic enzyme (20 μM in FAD) and phenosafranine redox dye (10 μM) were reduced by xanthine (200 μM), xanthine oxidase (100 nM), and benzyl viologen (2 μM) at pH 7.2 and 25 °C, according to Massey (*18*). (A) The spectra with decreasing absorbance were recorded at 0, 4, 8, 12, 16, 20, 24, 28, 32, 36, 40, and 44 min. (B) Log (ox/red) of dye versus log(ox/red) of enzyme-bound FAD. The reduction of phenosafranine was monitored by the decrease in absorbance at 520 nm, and the reduction of enzyme was monitored by the decrease in absorbance at 398 nm, allowing the ratios of oxidized and reduced species to be calculated. A midpoint potential of −258 mV for the phenosafranine couple at pH 7.2 (*19*) was used to determine the potential of the enzyme. The data yielded an enzyme midpoint potential of −237 ± 4 mV.

tions (diagrammed in Scheme 1). Scheme 1A shows the physiological NADH-CH_2-H_4folate oxidoreductase reaction. In the reductive half-reaction, the enzyme-bound FAD accepts reducing equivalents from the NADH substrate and becomes reduced. Measurement of the midpoint potential of the MTHFR-bound FAD yielded −237 mV at pH 7.2 (Figure 1). The midpoint potential for NADH/NAD^+ is −316 mV at pH 7.0 (*28*), and at pH 7.2, E_m is calculated to be −322 mV. The reduction of enzyme by NADH occurs with a difference in midpoint potential of 85 mV, which corresponds to a free energy decrease of −3.9 kcal mol^{-1}, and thus, the equilibrium for this half-reaction favors formation of reduced enzyme. In the oxidative half-reaction (Scheme 1A), the reduced FAD is reoxidized by transfer of reducing equivalents to CH_2-H_4folate. The midpoint potential for the CH_2-H_4folate/CH_3-H_4folate couple is −200 mV at pH 7.0 (*29*), and the E_m is calculated to be −212 mV at pH 7.2. From the respective potentials of the folate couple and the enzyme, a difference in midpoint potential of 25 mV at pH 7.2 can be calculated, which corresponds to a free energy change of −1.2 kcal mol^{-1}. Thus, this half-reaction is deemed reversible, and the enzyme can catalyze either of two half-reactions involving folate: reduction of CH_2-H_4folate as part

Scheme 1: MTHFR Assays and Half-Reactions

A. NADH-CH_2-H_4folate Oxidoreductase Assay

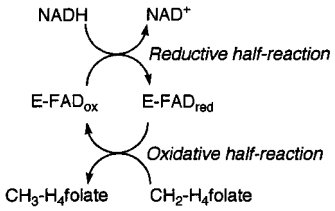

B. NADH-Menadione Oxidoreductase Assay

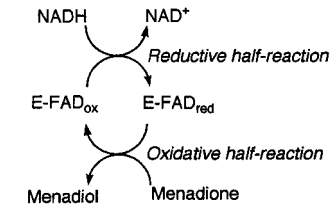

C. CH_3-H_4folate-Menadione Oxidoreductase Assay

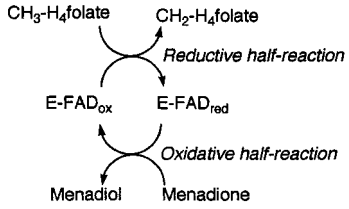

of the physiological oxidoreductase reaction (Scheme 1A) or oxidation of CH_3-H_4folate as part of the CH_3-H_4folate-menadione oxidoreductase reaction (Scheme 1C).

In the NADH-menadione (Scheme 1B) and CH_3-H_4folate-menadione (Scheme 1C) oxidoreductase assays, menadione is used as a high potential electron acceptor to return the flavin to its oxidized form. As will be discussed below, the rate constant associated with the reoxidation of reduced enzyme by menadione is very fast, and in both of these assays, the reductive half-reaction is rate limiting. Thus, under steady-state conditions, the NADH-menadione oxidoreductase assay examines the reduction of oxidized enzyme by NADH in the absence of the folate substrate, and the CH_3-H_4folate-menadione oxidoreductase assay examines the reduction of oxidized enzyme by CH_3-H_4folate in the absence of pyridine nucleotide.

For each oxidoreduction in Scheme 1, we have determined the steady-state kinetic parameters. Also, we have directly measured the net rate constants for reduction or oxidation of flavin in each half-reaction as a function of substrate concentration, using a stopped-flow spectrophotometer. Then, for each oxidoreductase reaction, a comparison has been made between the steady-state turnover number and that which would be calculated from the net rate constants of the respective half-reactions. As described below, this comparison allows the rate-limiting portions of each overall catalytic reaction to be ascertained.

Scheme 2 diagrams the kinetic constants associated with the reductive and oxidative half-reactions of the physiological oxidoreductase reaction and the constants corresponding to the oxidative half-reaction with menadione. Using the method of partition analysis and the concept of net rate constants

Scheme 2: Kinetic Mechanisms for MTHFR Hal-Reactions

$$E_{ox} + NADH \underset{k_{-1}}{\overset{k_1}{\rightleftharpoons}} E_{ox}\cdot NADH \underset{k_{-2}}{\overset{k_2}{\rightleftharpoons}} E_{red}\cdot NAD^+ \underset{k_{-3}}{\overset{k_3}{\rightleftharpoons}} E_{red} + NAD^+$$

$$E_{red} + CH_2\text{-}H_4folate \underset{k_{-4}}{\overset{k_4}{\rightleftharpoons}} E_{red}\cdot CH_2\text{-}H_4folate \underset{k_{-5}}{\overset{k_5}{\rightleftharpoons}} E_{ox}\cdot CH_3\text{-}H_4folate \underset{k_{-6}}{\overset{k_6}{\rightleftharpoons}} E_{ox} + CH_3\text{-}H_4folate$$

$$E_{red} + menadione \underset{k_{-7}}{\overset{k_7}{\rightleftharpoons}} E_{ox} + menadiol$$

developed by Cleland (*30*), the net rate constant k_2', which corresponds to the rate constant for the reductive half-reaction measured in the stopped-flow instrument, is given by eq 8.

$$k_2' = \frac{k_2 k_3}{k_{-2} + k_3} \tag{8}$$

As eq 8 reveals, the net rate constant k_2' does not provide information about the magnitude of k_3, the rate constant corresponding to product release, relative to k_2, the rate constant corresponding to enzyme reduction, and k_3 and/or k_2 may limit the value of k_2'. For comparison, the catalytic constant k_{cat} measured in steady-state turnover under conditions where the reductive half-reaction is rate limiting, is given by eq 9.

$$k_{cat} = \frac{k_2 k_3}{k_2 + k_{-2} + k_3} \tag{9}$$

The net rate constant k_2' differs from k_{cat} by the absence of the k_2 term in the denominator, and k_{cat} is sensitive to the relative magnitudes of k_2 and k_3 provided that $k_{-2} \ll k_2 + k_3$. Thus, in our analyses that follow, where one half-reaction limits the rate of overall turnover, comparisons between the net rate constant for that half reaction and k_{cat} have been made to ascertain the rate-limiting portions of each oxidoreductase half-reaction. For example, a near equivalence between k_2' and k_{cat} indicates that $k_2 \ll k_{-2} + k_3$, which will be the case if $k_3 \gg k_2$.

Reduction of Enzyme by NADH. The reductive-half reaction with NADH was studied in a stopped-flow spectrophotometer under anaerobic conditions by mixing oxidized enzyme with various concentrations of NADH. The reduction of the enzyme-bound FAD was monitored at 450 nm and the reaction traces were fit to two exponential phases (Figure 2A). No initial lag in the reaction was observed. The observed rate constant for reduction (slower phase) exhibited a hyperbolic dependence on the concentration of NADH (inset to Figure 2A). A fit of the data to eq 4 yielded an apparent K_d for NADH of 32 ± 5 μM and a maximum observed rate constant (net rate constant k_2') of 55 ± 6 s^{-1} (Table 1). Similar results were obtained from two other sets of experiments.

At 550 or 650 nm, transient long wavelength charge-transfer absorbance was observed during the course of reduction. Figure 2B shows the stopped-flow traces at 550 nm obtained from the reaction of 50 μM enzyme with 25−600 μM NADH (after mixing). At NADH concentrations of 25−100 μM, the traces were clearly biphasic, with a rapid increase in absorbance followed by a slower decrease. At NADH concentrations of 300 and 600 μM, the fast phase

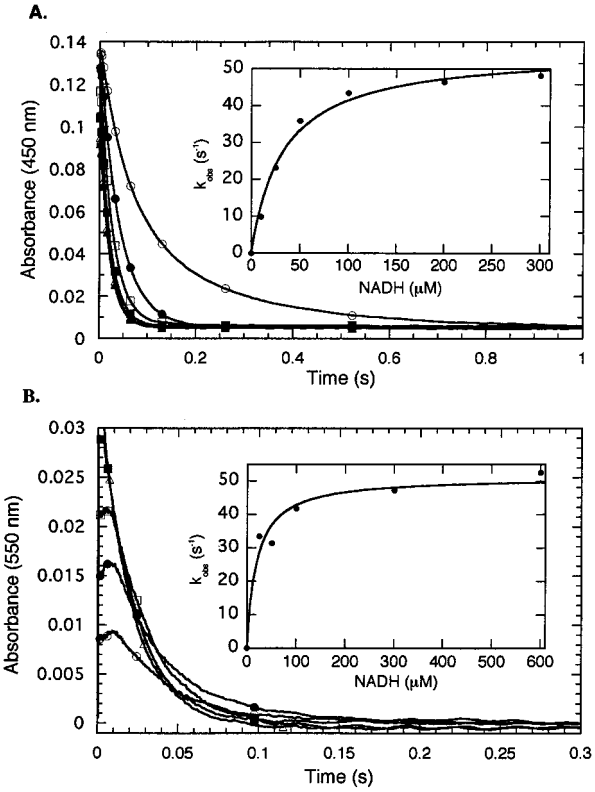

FIGURE 2: Reduction of enzyme by NADH. (A) Oxidized enzyme, 10 μM, was mixed with solutions of 10 (○), 25 (●), 50 (□), 100 (■), 200 (△), and 300 (▲) μM NADH (concentrations after mixing). Stopped-flow reaction traces, monitored at 450 nm, were fit to two exponential phases. Inset to panel A: dependence of the observed rate constant for reduction (slow phase) on NADH concentration. The data were fit to an hyperbolic equation (eq 4) which yielded an apparent K_d of 32 ± 5 μM for NADH and a maximum rate constant (k_2') of 55 ± 6 s^{-1}. (B). Charge-transfer interactions measured at 550 nm for the reaction of 50 μM enzyme with 25 (○), 50 (●), 100 (□), 300 (■), and 600 (△) μM NADH (concentrations after mixing) are shown. Inset to panel B: dependence of the observed rate constant for the slow phase at 550 nm on NADH concentration. The data were fit to eq 4 which yielded a maximum rate constant of 52 ± 3.3 s^{-1}.

was less apparent because it was complete within the dead time of the instrument. The observed rate constant for the slow phase at 550 nm showed a hyperbolic dependence on the concentration of NADH (inset to Figure 2B). Upon fitting the data to eq 4, the maximum observed rate constant was 52 ± 3.3 s^{-1} corresponding to the rate constant obtained for enzyme reduction at 450 nm. Taken together, the data at 450 and 550 nm are consistent with rapid formation of an E_{ox}-NADH charge-transfer complex followed by its decay, concomitant with reduction of the enzyme (*31*). The fast exponential phase observed at 450 nm is probably due to the small decrease at 450 nm that accompanies the formation

Table 1: Rapid-Reaction Kinetic Constants[a,b]

reductive half-reaction with NADH	
k_2' (s^{-1})	55 ± 6
K_d for NADH (μM)	32 ± 5
oxidative half-reaction with menadione	
k_7 (M^{-1} s^{-1})	$1.0 \times 10^7 \pm 0.3 \times 10^7$
at 140 μM (s^{-1}) (calcd)	1400 ± 500
oxidative half-reaction with CH_2-H_4folate	
k_5' (s^{-1})	10.3 ± 1.0
K_d for CH_2-H_4folate (μM)	11 ± 1
reductive half-reaction with CH_3-H_4folate	
k_{-5}' (s^{-1})	2.5 ± 0.5
K_d for CH_3-H_4folate (μM)	nd[c]

[a] Rate constants were determined at 25 °C in 50 mM potassium phosphate buffer (pH 7.2) containing 0.3 mM EDTA and 10% glycerol. [b] Values of rate constants were the average of two or three determinations. Definition of rate constants are given in Scheme 2. [c] Not determined.

Table 2: Steady-State Kinetic Constants[a,b]

NADH-menadione oxidoreductase assay	
k_{cat} (s^{-1})	55 ± 8.3
K_m for NADH (μM)	66 ± 16
K_i for NADH (μM)	12 ± 5
K_m for menadione (μM)	4 ± 1
NADH-CH_2-H_4folate oxidoreductase assay	
k_{cat} (s^{-1})	10.4 ± 1
K_m for NADH (μM)	20 ± 4
K_i for NADH (μM)	5 ± 2
K_m for CH_2-H_4folate (μM)	0.5 ± 0.1
K_i for CH_2-H_4folate (μM)	320 ± 25
CH_3-H_4folate-menadione oxidoreductase assay	
k_{cat} (s^{-1})	3.2 ± 0.4
K_m for CH_3−H_4folate (μM)	85 ± 9

[a] Kinetic constants were determined at 25 °C in 50 mM potassium phosphate buffer (pH 7.2) containing 0.3 mM EDTA and 10% glycerol. [b] Values of constants were the average of two to four determinations.

of the E_{ox}-NADH charge-transfer complex, as seen for *p*-hydroxybenzoate hydroxylase (*32*). The transient absorbance observed at 550 nm probably does not represent an E_{red}-NAD^+ charge-transfer complex; such a complex was not observed directly at 550 or 650 nm when photoreduced enzyme (10 μM) was reacted with solutions of up to 600 μM concentration NAD^+ (concentrations after mixing) in the stopped-flow instrument (data not shown).

Reoxidation of Reduced Enzyme by Menadione. As mentioned previously, MTHFR catalyzes the transfer of reducing equivalents from reduced bound FAD to menadione, an artificial electron acceptor. This half-reaction, utilized in both the NADH-menadione (Scheme 1B) and CH_3-H_4folate-menadione (Scheme 1C) assays, was examined in a stopped-flow apparatus. Reduced enzyme was prepared by photoreducing anaerobic, oxidized enzyme in the presence of EDTA and 5-deazaflavin (*23*). The reoxidation of photoreduced enzyme by menadione was monitored at pH 7.2 and 25 °C by measuring the increase in flavin absorbance at 450 nm (data not shown). When 10 μM reduced enzyme was mixed with solutions of menadione at concentrations ranging from 50 to 335 μM (after mixing), the enzyme was completely oxidized within the 3 ms dead time of the stopped-flow instrument. Only at menadione concentrations of less than 50 μM, could reoxidation of the enzyme be observed. From these data, an *approximate* second-order rate constant (k_7 in Scheme 2) of $1.0 \times 10^7 \pm 0.3 \times 10^7$ M^{-1} s^{-1} was estimated (Table 1). At a menadione concentration of 140 μM, therefore, the pseudo-first-order rate constant for the enzyme reoxidation would be 1400 ± 500 s^{-1}. For comparison, in the stopped-flow apparatus, the observed pseudo-first-order rate constant for oxidation of enzyme by oxygen-saturated buffer was approximately 0.06 s^{-1} (data not shown). Thus, reoxidation of enzyme by menadione occurs more than 20,000-fold faster than reoxidation by air.

NADH-Menadione Oxidoreductase Assay. The NADH-menadione oxidoreductase steady-state reaction consists of the two half-reactions described above: a reductive half-reaction, in which the flavin is reduced by NADH, and an oxidative half-reaction, in which the reduced flavin is reoxidized by menadione (diagrammed in Scheme 1B). The assay was carried out aerobically under steady-state conditions varying first menadione and then NADH. The menadione concentration was varied from 5 to 140 μM, while the NADH concentration was kept constant at 125 μM NADH (data not shown). Saturation was observed at approximately 50 μM menadione and a fit of the data to the Michaelis−Menten equation (eq 5) gave a K_m for menadione of 4 ± 1 μM (Table 2) and a maximum turnover number of 50 ± 5 s^{-1}. The low K_m value for menadione simply reflects the fact that the menadione half-reaction is not rate limiting when menadione concentrations are high, and reminds us that K_m values are often not K_d values. Using this assay, the NADH concentration was also varied from 10 to 300 μM in the presence of 140 μM menadione (Figure 3). At NADH concentrations greater than 200 μM, excess substrate inhibition was observed, as is characteristic of enzymes that follow ping-pong kinetic mechanisms (*33*). To correct the kinetic constants for the excess substrate inhibition, the data in Figure 3 were fit to eq 6 for single substrate inhibition in a ping-pong Bi−Bi system using Kaleidagraph. Employing 140 μM as the concentration of menadione (B) and 4 μM as the K_{mB} for menadione, the K_{mA} for NADH (A) was calculated to be 66 ± 16 μM, K_{iA} for NADH was 12 ± 5 μM, and the maximum turnover number (k_{cat}) was 55 ± 8.3 s^{-1} (Table 2). This observed steady-state turnover number for the NADH-menadione oxidoreductase reaction is in good agree-

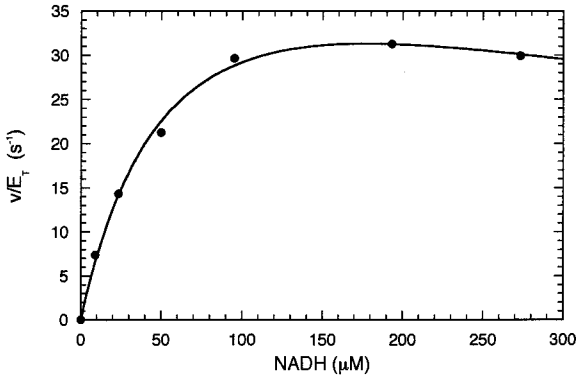

FIGURE 3: Enzyme activity in the NADH-menadione oxidoreductase assay. The assay was carried out aerobically in the presence of the indicated concentrations of NADH and 140 μM menadione. The reactions were initiated by the addition of enzyme to a final concentration of 16.7 nM. The dependence of v/E_T on the concentration of NADH is shown. Inhibition is evident at NADH concentrations above 100 μM. The data were fit to a single substrate inhibition equation (eq 6), which yielded a K_{mA} for NADH of 66 ± 16 μM, a K_{iA} for NADH of 12 ± 5 μM, and a k_{cat} of 55 ± 8.3 s^{-1}.

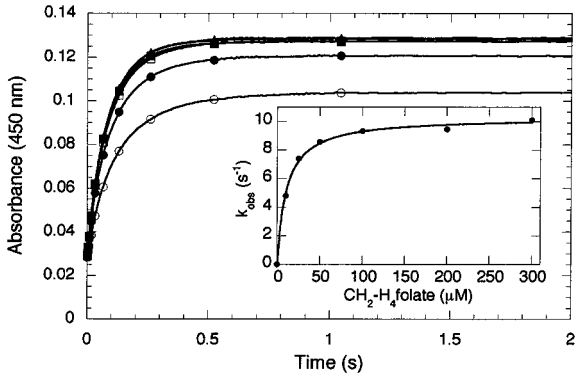

FIGURE 4: Reoxidation of reduced enzyme by CH_2-H_4folate. Photoreduced enzyme (10 μM) was mixed with solutions of 10 (○), 25 (●), 50 (□), 100 (■), 200 (△), and 300 (▲) μM CH_2-H_4folate (concentrations after mixing). Stopped-flow reaction traces were monitored at 450 nm. The reaction was biphasic. The fast and slow phases accounted for 25 and 75%, respectively, of the observed absorbance changes. Inset: Dependence of the observed rate constant for the slow phase on CH_2-H_4folate concentration. The data were fit to eq 4 which yielded an apparent K_d of 11 ± 1 μM for CH_2-H_4folate and a k_5' of 10.3 ± 1.0 s^{-1}.

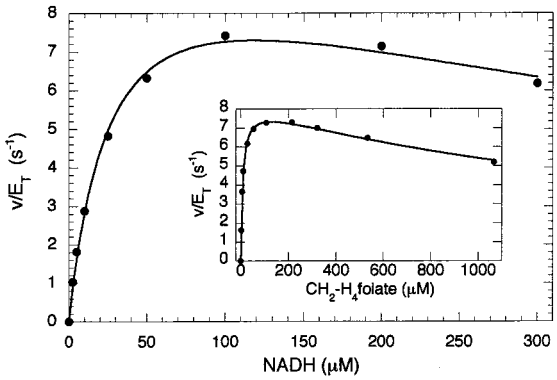

FIGURE 5: Measurement of turnover in the NADH-CH_2-H_4folate oxidoreductase assay. In a stopped-flow spectrophotometer, anaerobic enzyme (1.25 μM) was mixed with a solution containing 200 μM CH_2-H_4folate and 2.5−300 μM NADH (concentrations after mixing). The initial velocity, measured as the rate of oxidation of NADH at 340 nm, is plotted against the NADH concentration. (Inset) Plot of initial velocity vs CH_2-H_4folate concentration. Enzyme (1.25 μM) was mixed with solutions containing 100 μM NADH and 2−1000 μM CH_2-H_4folate (concentrations after mixing). Marked inhibition by substrate is evident for both NADH and CH_2-H_4folate substrates. Using eq 7, the solid-line fits to the data were determined, yielding the following kinetic parameters: K_{mA} for NADH of 20 ± 4 μM, K_{iA} for NADH of 5 ± 2 μM, K_{mB} for CH_2-H_4folate of 0.5 ± 0.1 μM, K_{iB} for CH_2-H_4folate of 320 ± 25 μM, and k_{cat} of 10.4 ± 1.0 s^{-1}.

ment with the expected value for the turnover number that can be calculated from the maximum first-order rate constants of the two half-reactions at saturating menadione (Figure 2, Table 1), assuming a ping-pong Bi−Bi mechanism (*34*).

$$\frac{v}{E_T} = \frac{k_2' k_7}{k_2' + k_7}\ s^{-1} = \frac{(55.0)(1400)}{(55.0 + 1400)}\ s^{-1} = 53\ s^{-1} \qquad (10)$$

Our analysis demonstrates that the reductive half-reaction with NADH (k_2') is rate limiting in the NADH-menadione oxidoreductase reaction. Furthermore, the agreement of calculated and observed turnover numbers suggests that the enzyme-catalyzed reaction follows a ping-pong kinetic pattern and that product release (k_3 in Scheme 2) is at least 10-fold faster than the rate of enzyme reduction (k_2), i.e., that the chemistry of reduction is rate limiting. The stopped-flow kinetics of the reductive half-reaction also support a mechanism where enzyme reduction is followed by fast release of the NAD product. Thus, steady-state studies of the NADH-menadione oxidoreductase reaction can be used to probe directly the chemical events associated with the NADH-linked reductive half-reaction.

Reoxidation of Reduced Enzyme by CH_2-H_4folate. The reoxidation of photoreduced enzyme by CH_2-H_4folate was monitored by measuring the increase in flavin absorbance at 450 nm in a stopped-flow spectrophotometer. Spectra taken after each shot indicated that full reoxidation had been achieved at CH_2-H_4folate concentrations after mixing of 50−300 μM, but not at 10 and 25 μM (data not shown). This difficulty in achieving full reoxidation at the lower substrate concentrations reflects the fact that the reaction proceeds to equilibrium rather than to completion under these conditions. A representative experiment is shown in Figure 4. The reaction traces were best fit to two exponential phases. The slow phase, accounting for 75% of the total absorbance change, showed a hyperbolic dependence on the concentration of CH_2-H_4folate (inset to Figure 4). Applying the data to eq 4, the apparent K_d for CH_2-H_4folate and the maximum observed rate constant for reoxidation (net rate constant k_5') were determined to be 11 ± 1 μM and 10.3 ± 1.0 s^{-1}, respectively (Table 1). The smaller, faster phase of the reaction accounted for 25% of the total absorbance change, demonstrated a hyperbolic dependence on CH_2-H_4folate concentration, and a maximum observed rate constant of 34 ± 3 s^{-1} was calculated. The origin of this fast phase is not known; it might be attributed to the rapid formation of a reduced enzyme-CH_2-H_4folate charge-transfer complex prior to enzyme reoxidation. In an attempt to observe such a complex, the oxidative half-reaction with CH_2-H_4folate was investigated at wavelengths 300, 500, and 550 nm in addition to 450 nm. No changes in absorbance were detected at 300 and 550 nm, although enzyme-CH_2-H_4folate charge-transfer complexes would be expected to absorb at 550 nm. At 500 nm, the traces were fit to two exponential phases and yielded rate constants similar to those obtained from the 450 nm traces (data not shown).

NADH-CH_2-H_4folate Oxidoreductase Assay. The physiological steady-state reaction is diagrammed in Scheme 1A. Because of the susceptibility of CH_2-H_4folate to oxidation, a steady-state analysis of the physiological reaction was carried out under anaerobic conditions in a stopped-flow spectrophotometer. Enzyme (1.25 μM after mixing) was mixed with an equal volume of a solution containing both NADH and CH_2-H_4folate. Figure 5 shows how the initial rate of NADH oxidation at 340 nm depends on NADH concentration over the range of 2.5−300 μM when CH_2-H_4folate was kept constant at a saturating concentration of 200 μM (concentrations after mixing). The inset to Figure 5 shows data from an experiment in which CH_2-H_4folate was varied from 2 to 1000 μM at an NADH concentration of 100 μM. Marked inhibition was seen at high concentrations of each substrate. Thus, the kinetic constants were determined by fitting the data to eq 7 by successive iterations using the program Kaleidagraph. K_{mA} for NADH (A) was calculated to be 20 ± 4 μM, K_{iA} for NADH (A) was 5 ± 2 μM, K_{mB}

for CH_2-H_4folate (B) was 0.5 ± 0.1 μM, and K_{iB} for CH_2-H_4folate was 320 ± 25 μM (Table 2). The maximum turnover number (k_{cat}) for the wild-type enzyme was determined to be 10.4 ± 1.0 s^{-1}. This number is in agreement with the theoretical turnover number that can be calculated from the maximum observed rate constants of the two half-reactions (Table 1), assuming a ping-pong Bi−Bi mechanism (*34*).

$$\frac{v}{E_T} = \frac{k'_2 k'_5}{k'_2 + k'_5}\ s^{-1} = \frac{(55.0)(10.3)}{(55.0 + 10.3)}\ s^{-1} = 8.7\ s^{-1} \quad (11)$$

Our analysis has demonstrated that of the two half-reactions constituting the physiological reaction, the oxidative half-reaction involving CH_2-H_4folate is more rate limiting in overall turnover than the reductive half-reaction involving NADH (see Scheme 2).

Reduction of Enzyme by CH_3-H_4folate. As mentioned previously, the reaction of enzyme-bound reduced flavin with CH_2-H_4folate occurring in the physiological direction is a reversible half-reaction (free energy change of −1.2 kcal/mol at pH 7.2 and 25 °C). Therefore, the reaction of oxidized enzyme with CH_3-H_4folate could be observed in a stopped-flow apparatus. The traces were fit to monophasic exponential curves (data not shown), yielding a maximum observed rate constant for reduction (net rate constant k'_{-5}) of 2.5 ± 0.5 s^{-1} at saturating CH_3-H_4folate (Table 1).

CH_3-H_4folate-Menadione Oxidoreductase Assay. The CH_3-H_4folate-menadione oxidoreductase reaction is shown in Scheme 1C. The steady-state assay was performed aerobically in the presence of saturating menadione (140 μM) and varying concentrations of CH_3-H_4folate. The data were fit to eq 5 and yielded a K_m for CH_3-H_4folate of 86 ± 2 μM and a maximum turnover number of 3.2 ± 0.4 s^{-1} (Table 2). This turnover number agrees reasonably with an expected value of 2.5 s^{-1} calculated from the maximum observed rate constants of the two half-reactions (Table 1). Our results indicate that reduction of enzyme by CH_3-H_4folate is rate limiting in the CH_3-H_4folate-menadione oxidoreductase reaction. The similarity between k_{cat} measured in steady-state turnover and k'_{-5} measured in the stopped-flow instrument suggests that the chemistry of reduction is rate limiting and that the product release is at least 10-fold faster than the rate of enzyme reduction. The monophasic stopped-flow kinetics of the reductive half-reaction is again consistent with a mechanism in which rate-limiting enzyme reduction is followed by fast release of the CH_2-H_4folate product.

DISCUSSION

We have determined the midpoint potential for the enzyme-bound FAD of *E. coli* MTHFR to be −237 mV at pH 7.2 and 25 °C. For comparison, FAD free in solution has a E_{m7} of −219 mV (*15*) and the E_m at pH 7.2 is calculated to be −231 mV. This 6 mV decrease in the midpoint potential for the MTHFR-bound FAD suggests that the enzyme environment surrounding the FAD slightly disfavors its reduction and this notion is supported by site-directed mutagenesis studies of aspartate and glutamate active site residues reported in the following paper in this issue (*35*). Here, we employed a redox dye method developed by Massey (*18*) to measure the −237 mV midpoint potential for the MTHFR enzyme. We have also determined the enzyme midpoint potential by titration of oxidized enzyme with CH_3-H_4folate under anaerobic conditions and analyses of oxidized and reduced enzyme and folate concentrations using the Nernst equation as described previously (*36*). This method yielded an enzyme midpoint potential of −223 mV (data not shown), 14 mV less negative than that determined using the redox dye procedure. A plausible explanation for this difference is tighter binding of CH_2-H_4folate to the reduced enzyme compared to the oxidized enzyme. This differential binding would force the equilibrium of the reaction to the right and make the enzyme reduction appear more favorable. Significantly, measurement of the porcine MTHFR midpoint potential using the titration method also yielded −223 mV (*12*), indicating that the redox properties of the bacterial and mammalian enzymes are quite similar.

In stopped-flow kinetic studies of the individual half-reactions catalyzed by *E. coli* MTHFR, we have shown that in all cases the half-reactions occur at rates sufficiently rapid to account for overall turnover (Table 1). Our analyses have demonstrated that the reduction of MTHFR by NADH proceeds in the absence of folate derivatives and that the reoxidation of reduced MTHFR by CH_2-H_4folate or the reduction of oxidized MTHFR by CH_3-H_4folate proceeds in the absence of bound NADH. These results are consistent with a ping-pong Bi−Bi kinetic mechanism for the enzyme. Direct spectrophotometric titrations of *E. coli* MTHFR with substrate (data not shown), as well as structural data revealing a single groove on the enzyme for the alternate binding of NADH or folate substrate (*8*), are also consistent with this mechanism, as are X-ray structures of the enzyme with bound analogues of each substrate (Martha Ludwig, personal communication). Furthermore, the excess substrate inhibition patterns observed in both the NADH-menadione (Figure 3) and NADH-CH_2-H_4folate (Figure 5) oxidoreductase assays are consistent with ping-pong Bi−Bi kinetics. In steady-state and rapid reaction studies on porcine MTHFR, the same kinetic mechanism was determined (*13*), suggesting that the bacterial and mammalian enzymes are indeed quite similar in their catalytic properties. This is an important similarity in support of our making use of the *E. coli* enzyme as a model for the less available mammalian enzyme.

We have shown that *E. coli* MTHFR is reduced by NADH with a maximum observed rate constant (k'_2) of 55 s^{-1} (Figure 2A) and the reduced enzyme is reoxidized by CH_2-H_4folate with a maximum rate constant (k'_5) of 10.3 s^{-1} (Figure 4). After correction for inhibition by NADH and by CH_2-H_4folate, the observed rate of turnover in the NADH-CH_2-H_4folate oxidoreductase reaction is 10.4 s^{-1} (Table 2), which is in reasonable agreement with the value predicted from the maximum rate constants of the two half-reactions (8.7 s^{-1}). These results indicate also that reoxidation of the flavin by CH_2-H_4folate is the rate-limiting half-reaction in the physiological reaction. Again, similar results were obtained with the porcine enzyme (*13*). These findings are not in agreement with those from our earlier paper (*9*) in which a maximum turnover number of 30 s^{-1} was reported and the reductive half-reaction was deemed rate limiting. In the earlier work, however, because of issues of enzyme stability, the physiological reaction was carried out at a higher enzyme concentration (10 μM after mixing) compared to the present analysis (1.25 μM after mixing) so that a true steady-

state rate of 10.4 ± 1 s^{-1} was not achieved. Thus, we believe that the rates of NADH oxidation reported in our earlier paper were measured during the approach to steady-state rather than during the steady-state stage of the reaction and, therefore, were overestimated. In the present work, the stability of the enzyme was extensively tested using the NADH-menadione and CH_3-H_4folate-menadione oxidoreductase assays; 2.5 μM enzyme was found to have the same activity at room temperature over a period of 6 h, conditions analogous to those employed during the physiological oxidoreductase experiments (data not shown).

After correction for inhibition by NADH, the observed rate of turnover in the NADH-menadione oxidoreductase reaction is 55 s^{-1} (Table 2). This value is in excellent agreement with the predicted value for turnover in this reaction (53 s^{-1}), calculated from the observed first-order rate constants for flavin reduction by NADH (55 s^{-1}) and for flavin reoxidation by 140 μM menadione (1400 s^{-1}). The NADH-linked reductive half-reaction is, therefore, nearly fully rate limiting in this oxidoreduction. We have also demonstrated that reduction of flavin by CH_3-H_4folate is nearly fully rate limiting in the CH_3-H_4folate-menadione oxidoreductase reaction. Taken together, these results indicate that steady-state kinetic studies of the NADH-menadione and CH_3-H_4folate-menadione oxidoreductase assays can be used to investigate events associated with flavin reduction by NADH and with flavin reduction by CH_3-H_4folate, respectively. Moreover, based on our measured rate constant for the reaction of oxygen with reduced MTHFR (0.06 s^{-1}) compared to that for menadione (1400 s^{-1}), it is very reasonable to carry out assays with menadione aerobically.

When *E. coli* MTHFR is reacted with NADH in the stopped-flow spectrophotometer, reaction traces observed at 550−650 nm are biphasic, indicating formation and decay of a charge-transfer complex (Figure 2). Taken together, our results are consistent with the rapid formation of an oxidized enzyme-NADH charge-transfer complex followed by its decay, concomitant with reduction of the flavin. Our stopped-flow measurements of k'_2, which are in agreement with the k_{cat} measurements during steady-state turnover of the NADH-menadione oxidoreductase reaction, demonstrate that in Scheme 2, $k'_2 \ll k_7$ i.e., the reductive half-reaction is rate limiting in overall turnover. The kinetic expressions for k'_2 and k_{cat} are shown above in eqs 8 and 9, respectively. The agreement between k'_2 and k_{cat} suggests that in the reductive half-reaction, $k_3 \gg k_2$, i.e., NAD^+ product release is at least 10-fold faster than flavin reduction. Rate-limiting enzyme reduction followed by fast product release is also consistent with the observed kinetics in the stopped-flow instrument. A similar analysis applies to the reduction of MTHFR by CH_3-H_4folate in the CH_3-H_4folate-menadione oxidoreductase reaction. The reduction of flavin by CH_3-H_4folate is rate limiting in the assay. The monophasic kinetics observed in the stopped-flow apparatus for the reductive half-reaction and the similar calculated and measured k_{cat} values are consistent with a mechanism whereby enzyme reduction is followed by fast release of the CH_2-H_4folate product.

In the stopped-flow instrument, oxidation of reduced enzyme by CH_2-H_4folate was biphasic at 450 nm and both the slow and fast phases showed a hyperbolic dependence on CH_2-H_4folate concentration (Figure 4). One of our referees suggested two mechanisms to account for the biphasic kinetics. The first involves formation of a spectrally distinct intermediate from the E_{red}·CH_2-H_4folate Michaelis complex prior to hydride transfer. A plausible intermediate in our reaction would be a charge-transfer complex between the reduced flavin and the oxidized substrate. Such complexes typically have broad low intensity absorbance between 500 and 800 nm and absorbance typical of reduced flavin between 350 and 500 nm. For example, Beaty and Ballou have shown such a species with the flavin monooxygenase from pig liver (*37*). However, as noted in results, we could not detect any such intermediate.

The second possibility is that an equilibrium is established between E_{red}·CH_2-H_4folate and E_{ox}·CH_3-H_4folate prior to the rate-limiting release of CH_3-H_4folate. In this case the apparent rate constant for the fast phase would correspond to $k_5 + k_{-5}$ (rate constants in Scheme 2) and that for the slow phase would be k_6. During NADH-CH_2-H_4folate oxidoreductase turnover, the net rate constant for reduction of the flavin by NADH (55 s^{-1}) is much greater than k_{cat} (10 s^{-1}), indicating that the oxidative half reaction is rate limiting in turnover. Moreover, the net rate constant (k'_5) for the slow phase of the oxidative half reaction is the same as k_{cat}. The observed rate constants for the oxidative half reaction and for overall catalysis are given by equations 12 and 13.

$$k'_5 = \frac{k_5 k_6}{(k_{-5} + k_6)} \tag{12}$$

$$k_{cat} = \frac{k_5 k_6}{(k_5 + k_{-5} + k_6)} \tag{13}$$

These relationships imply that $k_5 \ll k_{-5} + k_6$. Because the fast phase equilibrium accounts for ~17% of the amplitude, $5k_5 \sim k_{-5}$. The maximum observed rate constant for this first phase is 34 s^{-1}, so that $k_5 \sim 6$ s^{-1}, which is less than the observed rate constant for the oxidative half reaction. Thus it is unlikely that a preequilibrium model can account for the observed biphasic reactions.

The two simple explanations above are not adequate to explain these data. Alternate possibilities such as negative cooperativity between the subunits of the homotetrameric enzyme could underlie our observations. It is known that the enzyme can dissociate to form dimers at low concentrations (*8*). However, further experiments will be necessary to test such a proposal.

In this paper, we have characterized the kinetic mechanism of *E. coli* MTHFR. We have established that observations derived from study of the individual half-reactions are relevant to the overall oxidoreductase reactions catalyzed by the enzyme and that they, therefore, can be used to reach conclusions about the enzyme mechanism. Moreover, we have shown that the *E. coli* enzyme follows a ping-pong Bi−Bi kinetic mechanism very similar to that of the porcine enzyme, demonstrating that it is a good model for the mammalian enzyme. In the following paper, we probe the role of specific amino acid residues in the chemical mechanism of *E. coli* MTHFR by examining the properties of two mutant enzymes.

ACKNOWLEDGMENT

We thank Professor Vincent Massey (University of Michigan) for the gift of 3,10-dimethyl-5-deazaisoalloxazine

and xanthine oxidase and Eprova (Schaffhausen, Switzerland) for (6*S*)-H_4folate and (6*S*)-CH_3-H_4folate. We thank Vincent Massey, Mariliz Ortiz-Maldonado, L. David Arscott, Bruce Palfey, Christal Sheppard, and Vahe Bandarian for helpful discussions.

REFERENCES

1. Clarke, R., Daly, L., Robinson, K., Naughten, E., Cahalane, S., Fowler, B., and Graham, I. (1991) *New Engl. J. Med. 324*, 1149−1155.
2. Boushey, C. J., Beresford, S. A. A., Omenn, G. S., and Motulsky, A. G. (1995) *J. Am. Med. Assoc. 274*, 1049−1057.
3. Steegers-Theunissen, R. P. M., Boers, G. H. J., Trijbels, F. J. M., and Eskes, T. K. A. B. (1991) *New Engl. J. Med. 324*, 199−200.
4. Mills, J. L., McPartlin, J. M., Kirke, P. N., Lee, Y. J., Conley, M. R., Weir, D. G., and Scott, J. M. (1995) *Lancet 345*, 149−151.
5. van der Put, N. M., van der Molen, E. F., Kluijtmans, L. A., Heil, S. G., Trijbels, J. M., Eskes, T. K., Van Oppenraaij-Emmerzaal, D., Banerjee, R., and Blom, H. J. (1997) *Q. J. Med. 90*, 511−517.
6. Matthews, R. G. (1991) in *Chemistry and Biochemistry of Flavoenzymes* (Müller, F., Ed.) pp 371−387, CRC Press, Boca Raton.
7. Goyette, P., Sumner, J. S., Milos, R., Duncan, A. M. V., Rosenblatt, D. S., Matthews, R. G., and Rozen, R. (1994) *Nat. Genet. 7*, 195−200.
8. Guenther, B. D., Sheppard, C. A., Tran, P., Rozen, R., Matthews, R. G., and Ludwig, M. L. (1999) *Nat. Struct. Biol. 6*, 359−365.
9. Sheppard, C. A., Trimmer, E. E., and Matthews, R. G. (1999) *J. Bacteriol. 181*, 718−725.
10. Kutzbach, C., and Stokstad, E. L. R. (1971) *Biochim. Biophys. Acta 250*, 459−477.
11. Jencks, D. A., and Matthews, R. G. (1987) *J. Biol. Chem. 262*, 2485−2493.
12. Daubner, S. C., and Matthews, R. G. (1982) *J. Biol. Chem. 257*, 140−145.
13. Vanoni, M. A., Ballou, D. P., and Matthews, R. G. (1983) *J. Biol. Chem. 258*, 11510−11514.
14. Bull, C., and Ballou, D. P. (1981) *J. Biol. Chem. 256*, 12673−12680.
15. Fasman, G. D. (1976) *Handbook of Biochemistry and Molecular Biology*, Vol. I, 3rd ed., CRC Press, Inc., Cleveland, OH.
16. Dawson, R. M., Elliott, D. C., Elliott, W. H., and Jones, K. M. (1969) *Data for Biochemical Research*, Clarendon Press, Oxford.
17. Blakley, R. L. (1969) *The Biochemistry of Folic Acid and Related Pteridines*, North-Holland, Amsterdam.
18. Massey, V. (1991) in *Flavins and Flavoproteins 1990* (Curti, B., Ronchi, S., and Zanetti, G., Eds.) pp 59−66, Walter de Gruyter, Berlin.
19. Clark, W. M. (1960) *Oxidation−Reduction Potentials of Organic Systems*, Williams & Wilkins, Baltimore.
20. Williams, C. H., Jr., Arscott, L. D., Matthews, R. G., Thorpe, C., and Wilkinson, K. D. (1979) *Methods Enzymol. 62*, 185−98.
21. Minnaert, K. (1965) *Biochim. Biophys. Acta 110*, 42−56.
22. Patel, P., and Ballou, D. P. (2000) *Anal. Biochem. 286*, 187−192.
23. Massey, V., and Hemmerich, P. (1978) *Biochemistry 17*, 9−17.
24. Press, W. H., Teulosky, S. A., Vettering, W. T., and Flannery, B. P. (1992) *Numerical Methods in C*, 2nd ed., Cambridge University Press, Cambridge.
25. Donaldson, K. O., and Keresztesy, J. C. (1962) *J. Biol. Chem. 237*, 1298−1304.
26. Matthews, R. G. (1986) *Methods Enzymol. 122*, 372−381.
27. Cleland, W. W. (1979) *Methods Enzymol. 63*, 500−513.
28. Bergmeyer, H. (1988) *Methods of Enzymatic Analysis*, Vol. 2nd, 3rd ed., Verlag Chemie, Weinheim.
29. Wohlfarth, G., and Diekert, G. (1991) *Arch. Microbiol. 155*, 378−381.
30. Cleland, W. W. (1975) *Biochemistry 14*, 3220−3224.
31. Husain, M., and Massey, V. (1979) *J. Biol. Chem. 254*, 6657−6666.
32. Howell, L. G., Spector, T., and Massey, V. (1972) *J. Biol. Chem. 247*, 4340−4350.
33. Garces, E., and Cleland, W. W. (1969) *Biochemistry 8*, 633−640.
34. Massey, V., Gibson, Q. H., and Veeger, C. (1960) *Biochem. J. 77*, 341−351.
35. Trimmer, E. E., Ballou, D. P., Ludwig, M. L., and Matthews, R. G. (2001) *Biochemistry 40*, 6216−6226.
36. Daubner, S. C., and Matthews, R. G. (1982) in *Flavins and Flavoproteins* (Massey, V., and Williams, C. H., Eds.) pp 165−172, Elsevier, New York.
37. Beaty, N. P., and Ballou, D. P. (1981) *J. Biol. Chem. 256*, 4611−4618.

BI002789W